Hindawi
Mathematical Problems in Engineering
Volume 2021, Article ID 5548184, 14 pages
https://doi.org/10.1155/2021/5548184

Research Article

Design of Neutrosophic Self-Tuning PID Controller for AC Permanent Magnet Synchronous Motor Based on Neutrosophic Theory

Zhongliang Fu,[1,2] **Chunping Liu**,[3] **Shengyi Ruan**,[3] **and Kun Chen**[3]

[1]*Zhejiang Yili Auto Air-conditioner Co. Ltd., Lishui 323700, China*
[2]*Longquan Celadon Sword Technician College, Lishui 323700, China*
[3]*School of Mechanical and Electrical Engineering, Shaoxing University, Shaoxing 312000, China*

Correspondence should be addressed to Kun Chen; kchen@usx.edu.cn

Received 30 January 2021; Revised 15 April 2021; Accepted 29 April 2021; Published 12 May 2021

Academic Editor: Xiaodong Sun

In practical control applications, AC permanent magnet synchronous motors need to work in different response characteristics. In order to meet this demand, a controller which can independently realize the different response characteristics of the motor is designed based on neutrosophic theory and genetic algorithm. According to different response characteristics, neutrosophic membership functions are constructed. Then, combined with the cosine measure theorem and genetic algorithm, the neutrosophic self-tuning PID controller is designed. It can adjust the parameters of the controller according to response requirements. Finally, three kinds of controllers with typical system response characteristics are designed by using Simulink. The effectiveness of the designed controller is verified by simulation results.

1. Introduction

Compared with the traditional electric excitation synchronous motor, permanent magnet synchronous motor (PMSM) has the advantages of less loss, high efficiency, and low power consumption. It is excited by a permanent magnet. The structure is simple and the cost is low. The collector ring and brush are omitted, and the reliability is improved. The rotor does not need an excitation current. So, the excitation loss no longer exists. And the efficiency and power factor of the motor are improved. In recent years, the research and application of PMSM have been very popular [1]. It is meaningful to study the method to make PMSM work effectively on the demand response characteristics.

In fact, some parameters of the system are not constants but will change with time, such as manufacturing tolerances, aging of major components, and environmental changes. This will affect the control performance to a certain extent. In order to improve the control performance of the PMSM, Sun et al. [2] proposed an improved MPCC scheme for PMSM drives to overcome the high torque and current ripples. At the same time, the steady-state and dynamic performance of PMSM drives are further improved. In [3], a new method to extract accurate rotor position for the speed sensorless control of surface-mounted permanent magnet synchronous motors (SPMSMs) based on the back electromotive force (EMF) information is presented. In [4], a novel method for the sensorless control of interior permanent magnet synchronous motors is proposed. An iterative search strategy based on dichotomy is proposed to provide a finite number of rotor position angles with good accuracy. Hussein [5] proposed a variety of uncertainty system modeling methods and robust stability analysis methods for interval linear time invariant systems. Hote et al. [6] introduced the robust stability analysis of the PWM push-pull DC-DC converter. Then, Precup and Preitl [7] proposed the integral servo system with proportional integral (PI) and proportional integral derivative (PID)

controllers to ensure stability and robustness of the controller. Elkaranshawy et al. [8] designed the PID robust controller of flexible arm robot by using the Kharitonov theorem.

In order to further solve the problems of uncertainty and inconsistent information, the concept of neutrosophic set was first proposed by Smarandache [9]. Then, the neutrosophic theory developed rapidly. Wang et al. [10] proposed the single valued neutrosophic set. Ye [11] further proposed the concept of a simplified neutrosophic set, including the concepts of single valued neutrosophic set and interval neutrosophic set. Subsequently, researchers have solved many practical engineering problems based on the theory of neutrosophic set, such as fault diagnosis [12, 13], Multiattribute group decision making [14, 15], linear and nonlinear programming [16], linear equation of traffic flow [17], and roughness coefficient of rock discontinuity [18].

PID algorithm is the most widely used in the field of engineering control. But the tuning of PID parameters is a tedious process. At present, the PID tuning methods studied by scholars include genetic algorithm [19], particle swarm optimization [20], and fuzzy control algorithm [21]. The tuning of PID parameters based on neutrosophic theory was proposed by Can and Ozguven [22]. However, it uses a traversal search algorithm, and the precision and speed cannot be considered at the same time. Ye [23, 24] proposed a cosine similarity measure. Combined with the genetic algorithm, the Can's PID tuning method is optimized. Ruan et al. [25] further extended and compared the neutrosophic PID tuning methods with cosine similarity measure, exponential similarity measure, and simulated annealing algorithm.

In this paper, the neutrosophic PID tuning control algorithm under different response characteristics is studied. Neutrosophic membership functions are constructed corresponding to different characteristics and the cosine measure theorem and genetic algorithm are used to tune the parameters and get the optimal values.

The paper is organized as follows. In Section 2, the PMSM model is described. And neutrosophic self-tuning PID controller is designed in Section 3. Simulations are shown in Section 4. Finally, the conclusion of this work is summarized in Section 5.

2. PMSM Model Description

2.1. Basic Equations of PMSM. PMSM control system is a high-order, nonlinear, multivariable strong coupling system, so its mathematical model contains time-varying parameters, and the magnetic circuit relationship is also complex.

The section coordinate diagram of PMSM is shown in Figure 1. The a-axis of the stationary coordinate system coincides with the A-phase winding, which is used to analyze the mathematical model of the PMSM.

2.1.1. Voltage Equation [26]. In the coordinate system, the voltage matrix equation of PMSM is as follows:

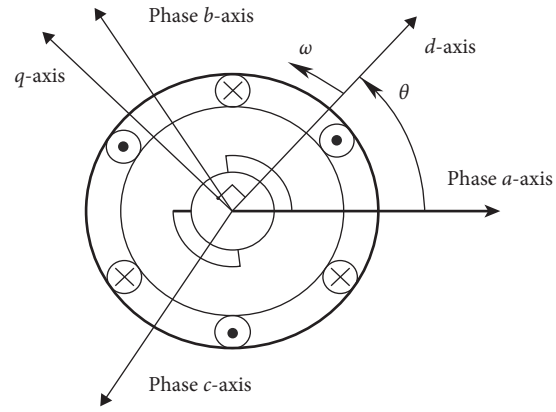

Figure 1: Schematic diagram of PMSM section coordinates.

$$\begin{bmatrix} u_a \\ u_b \\ u_c \end{bmatrix} = \begin{bmatrix} R_s & 0 & 0 \\ 0 & R_s & 0 \\ 0 & 0 & R_s \end{bmatrix} \begin{bmatrix} i_a \\ i_b \\ i_c \end{bmatrix} + p \begin{bmatrix} \varphi_a \\ \varphi_b \\ \varphi_c \end{bmatrix}, \tag{1}$$

where u_a,u_b, and u_c are the stator phase voltages, i_a, i_b, and i_c are the stator phase currents, φ_a, φ_b, and φ_c are stator flux, R_s is the stator resistance, and p is a differential operator.

The voltage equation of AC permanent magnet synchronous motor in the two-phase rotating $d-q$ coordinate system is derived as follows:

$$U_d = p\varphi_d - \omega\varphi_q + R_s i_d, \tag{2}$$

$$U_q = p\varphi_q - \omega\varphi_d + R_s i_q. \tag{3}$$

2.1.2. Flux Linkage Equation [27, 28]. The flux linkage equation of PMSM in the $d-q$ coordinate system is as follows:

$$\begin{bmatrix} \varphi_d \\ \varphi_q \end{bmatrix} = \begin{bmatrix} L_d & 0 \\ 0 & L_q \end{bmatrix} \begin{bmatrix} i_d \\ i_q \end{bmatrix} + \varphi_r \begin{bmatrix} 1 \\ 0 \end{bmatrix}, \tag{4}$$

where φ_r is rotor flux linkage and L_d and L_q are as follows:

$$L_d = L_1 - M_1 + \frac{3}{2}(L_0 + L_2), \tag{5}$$

$$L_q = L_1 - M_1 + \frac{3}{2}(L_0 - L_2). \tag{6}$$

2.1.3. Electromagnetic Torque Equation. The power of PMSM is equal to the product of phase voltage and phase current of each phase. It can be expressed as follows:

$$\begin{aligned} P &= u_a i_a + u_b i_b + u_c i_c \\ &= \frac{3}{2}\left(u_d i_d + u_q i_q\right) \\ &= \frac{3}{2} P\ dq\ . \end{aligned} \tag{7}$$

After coordinate transformation, the power is changed in form, but its magnitude is 3/2 of the input power in the $d-q$ coordinate system. To further analyze the input power, the voltage equation is introduced into equation (7), and then the electromagnetic torque equation is obtained as follows:

$$T_e = \frac{3}{2}P_n\left(\varphi_d i_q - \varphi_q i_d\right) = \frac{3}{2}P_n\left[\varphi_f i_q - \left(L_q - L_d\right)i_d i_q\right], \quad (8)$$

where p_n is the pole number of the motor and φ_f is the flux linkage of the permanent magnet. Generally speaking, $L_d = L_q$ is satisfied.

2.1.4. Equation of Motion. The electromagnetic torque of PMSM not only drives the motor load but also overcomes the friction damping and inertia of the permanent magnet rotor. The torque balance formula is as follows:

$$T_e = T_L + \frac{J}{P_n}p\omega + \frac{\omega}{P_n}p + B\omega. \quad (9)$$

By integrating equations (2)–(4), (8), and (9), the mathematical model of three-phase AC PMSM can be obtained as follows:

$$p\begin{bmatrix} i_d \\ i_q \\ \omega \end{bmatrix} = \begin{bmatrix} -\frac{R_s}{L} & P_n & 0 \\ -P_n\omega & -\frac{R_s}{L} & -\frac{P_n\omega_f}{L} \\ 0 & \frac{(3/2)P_n\varphi_f}{J} & 0 \end{bmatrix}\begin{bmatrix} i_d \\ i_q \\ \omega \end{bmatrix} + \begin{bmatrix} \frac{u_d}{L} \\ \frac{u_q}{L} \\ -\frac{T_L}{J} \end{bmatrix}. \quad (10)$$

2.2. Vector Control Principle of PMSM. Since the mathematical model of PMSM is a nonlinear and strong coupling mathematical model, we need to use the vector control method to decouple the mathematical model. And combined with an appropriate control method, the speed control requirements can be achieved. The control method used in this paper is to make $i_d = 0$. More details can be found in [29, 30]. Then, the decoupling mathematical model can be obtained as follows:

$$p\begin{bmatrix} i_d \\ i_q \\ \omega \end{bmatrix} = \begin{bmatrix} P_n\omega & 0 \\ -\frac{R_s}{L} & -\frac{P_n\omega_f}{L} \\ \frac{(3/2)P_n\varphi_f}{J} & 0 \end{bmatrix}\begin{bmatrix} i_q \\ \omega \end{bmatrix} + \begin{bmatrix} \frac{u_d}{L} \\ \frac{u_q}{L} \\ -\frac{T_L}{J} \end{bmatrix}. \quad (11)$$

3. Design of Neutrosophic Self-Tuning PID Controller

3.1. Neutrosophic Theory. The variable X is defined as a universe of discourse. Any single-valued neutrosophic set N in X can be expressed as follows [31]:

$$N = \{(x, T_N(x), I_N(x), F_N(x) | x \in X)\}, \quad (12)$$

where $T_N(x)$ is a true membership function, $I_N(x)$ is an uncertain membership function, and $F_N(x)$ is a false membership function.

And each x satisfies the following conditions:

$$\begin{cases} T_N(x), I_N(x), F_N(x) \in [0,1], \\ 0 \le T_N(x) + I_N(x) + F_N(x) \le 3. \end{cases} \quad (13)$$

For convenience, $x = (T, I, F)$ is defined as a single-valued neutrosophic number in X.

Definition 1 (see [32]). If there are two neutrosophic sets N_1 and N_2 that belong to the universe of discourse $X = \{x_1, x_2, \ldots, x_n\}$, the specific forms are as follows:

$$\begin{cases} N_1 = \left\{\left(x_i, T_{N_1}(x_i), I_{N_1}(x_i), F_{N_1}(x_i) | x_i \in X\right)\right\}, \\ N_2 = \left\{\left(x_i, T_{N_2}(x_i), I_{N_2}(x_i), F_{N_2}(x_i) | x_i \in X\right)\right\}. \end{cases} \quad (14)$$

Then, the cosine similarity measure between N_1 and N_2 can be defined by

$$Cs(N_1, N_2) = \frac{1}{n}\sum_{i=1}^{n}\cos\left\{\frac{\pi}{6}\left[\left|T_{N_1}(x_i) - T_{N_2}(x_i)\right| + \left|I_{N_1}(x_i) - I_{N_2}(x_i)\right| + \left|F_{N_1}(x_i) - F_{N_2}(x_i)\right|\right]\right\}. \quad (15)$$

$Cs(N_1, N_2)$ has the following properties:

(1) $0 \le Cs(N_1, N_2) \le 1$

(2) If $N_1 = N_2$, then $Cs(N_1, N_2) = 1$

(3) $Cs(N_1, N_2) = Cs(N_2, N_1)$

(4) If N_3 is also a neutrosophicset belonged to X, and satisfies $N_1 \subseteq N_2 \subseteq N_3$, then $Cs(N_1, N_3) \leq Cs(N_1, N_2)$ and $Cs(N_1, N_3) \leq Cs(N_2, N_3)$ is established

3.2. Genetic Algorithm. The flowchart of the genetic algorithm is shown in Figure 2. Initialization includes generation population size, determination of iteration times, coding, selection, crossover, mutation probability, etc. The criterion for judging whether to end is to specify the number of iterations or to specify your own ending criteria, such as the emergence of a more suitable individual. In addition, it is possible to use decimal number operations directly without encoding and decoding. There are many pieces of research on genetic algorithms, which will not be repeated here.

3.3. Neutrosophic Self-Tuning PID Control Method. This paper will adopt the PID control algorithm, which is very effective in engineering. In particular, the incremental PID is only related to the last three errors, which greatly improves the stability of the system. Its specific form is as follows [33]:

$$\Delta u_k = Ae_k - Be_{k-1} + Ce_{k-2}, \tag{16}$$

where Δu_k is the control signal. A, B, and C are parameters. More details can be found in [33].

The PID parameter self-tuning method is designed based on the neutrosophic theory and genetic algorithm. The self-tuning method needs to consider multiple system response characteristics, that is, a multiobjective programming model problem. In order to comprehensively investigate the advantages and disadvantages of a system, we choose rising time, settling time, peak time, overshoot ratio, undershoot ratio, and steady-state error as the transient characteristics of the control system. According to different response characteristics, neutrosophic membership functions are constructed. Finally, the cosine similarity measure method is used to calculate the measurement value between the transient characteristics and the ideal response characteristics.

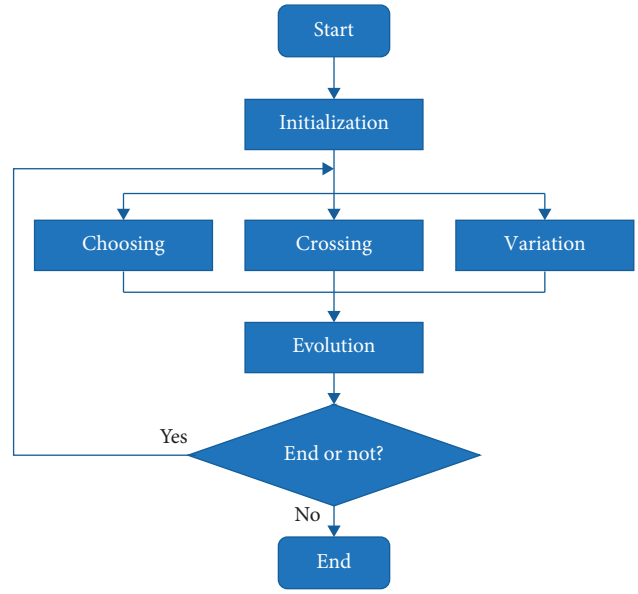

Figure 2: The flowchart of the genetic algorithm.

The triangular and trapezoidal membership functions are adopted for neutrosophic processing. The six transient characteristics are taken as a whole feature set $S = \{S_1, S_2, S_3, S_4, S_5, S_6\}$. In the set S, element S_1 means the rising time, S_2 means the settling time, S_3 means the peak time, S_4 means the overshoot ratio, S_5 means the undershoot ratio, and S_6 means the steady-state error.

Using the neutrosophic theory, the following form is given:

$$N = \{\langle S_1, T_1, I_1, F_1\rangle, \langle S_2, T_2, I_2, F_2\rangle, \langle S_3, T_3, I_3, F_3\rangle, \langle S_4, T_4, I_4, F_4\rangle, \langle S_5, T_5, I_5, F_5\rangle, \langle S_6, T_6, I_6, F_6\rangle\}, \tag{17}$$

and the ideal N^* is shown as follows:

$$N^* = \{\langle S_1, 1, 0, 0\rangle, \langle S_2, 1, 0, 0\rangle, \langle S_3, 1, 0, 0\rangle, \langle S_4, 1, 0, 0\rangle, \langle S_5, 1, 0, 0\rangle, \langle S_6, 1, 0, 0\rangle\}. \tag{18}$$

Then, using cosine similarity measure, we can get the similarity of N and N^* as follows:

$$C(N, N^*) = \frac{1}{n}\sum_{i=1}^{n} \cos\left\{\frac{\pi}{6}\left[\left|T_N(x_i) - T_{N^*}(x_i)\right| + \left|I_N(x_i) - I_{N^*}(x_i)\right| + \left|F_N(x_i) - F_{N^*}(x_i)\right|\right]\right\}. \tag{19}$$

The rule of PID parameter self-tuning is to minimize $[1 - C(N, N^*)]$.

The structure diagram of control system is shown in Figure 3. The inner loop of the control system is current loop and the outer loop is speed loop.

Remark 1. The main feature of this control system is that the neutrosophic self-tuning PID control method can realize the control of PMSM with different response characteristics. What users need to do is to give the response characteristics they want by simply adjusting the membership function. Cosine similarity measure method and genetic algorithm in the control system can find the optimal parameters of PID controller automatically, instead of manual adjustment.

4. Simulations

4.1. Simulink Module Building. In order to facilitate observation in the Simulink module, the main system is first established as shown in Figure 4. The speed, angle, torque, and current of L_d and L_q can be displayed in the scope. Powergui sets the working frequency of the whole system, which is equivalent to the CPU working frequency of 20 microseconds. The sampling time of each sensor is different, which can be represented by different zero-order holders. Then the subsystem as shown in Figure 5 is built to assemble the core module.

This is a double loop system. The inner loop is the current loop and the outer loop is the velocity loop. The sampling speeds of the angle sensor and speed sensor are set to 1 ms. The speed of the current sensor is faster, set to 0.2 ms. In order to be close to reality, the random white noise is added to the speed sensor with the amplitude of ±0.1 rad/s. The data of the speed sensor are processed by a sliding filter. The average value of five sampling data is taken as the measured value of actual speed. The sampling time of each sensor can be adjusted according to the actual situation.

The two-phase DC to three-phase AC module is shown in Figure 6. The operations in each submodule are slightly different. The angle offset of the first, second, and third modules in Figures 7–9 are 0, −120, and 120, respectively.

The PMSM used in this simulation is shown in Figure 10. The specific parameter settings are shown in Table 1.

4.2. Scheme. The simulations are divided into three parts: nonovershooting system, fast response system, and comprehensive response system.

4.2.1. Nonovershooting System. The nonovershooting system expects no overshoot in the response process. The design process of the overshoot ratio neutrosophic membership function should meet the following principles.

The parameters of the true, false, and uncertain membership functions should be selected in the range of small overshoot ratio. The smaller the overshoot requirement is, the larger the true value should be. The larger the overshoot requirement is, the larger the false value should be. The system has relatively low requirements for the other five characteristics. So the neutrosophic membership functions are designed as shown in Figure 11.

The desired speed is u_d = 5rad/s. The simulation results are shown in Figure 12 and Table 2. It can be seen from Figure 12 that the speed can converge to 5 rad/s. There is no overshoot in the response process of the rotor speed. In Table 2, the overshoot ratio of the response curve is 0% and the control objective without overshoot is satisfied.

The iteration of the group in the simulation is shown in Figure 13. The red circle is the best individual in each generation, and the blue star is the average value of each generation. It can be seen from Figure 13 that the overall trend is downward. The red curve is convergent and finally stabilizes at 0.0951.

4.2.2. Fast Response System. The fast response system expects fast response speed. So, the rising time and peak time should be short, and the overshoot and undershoot ratio can be appropriately increased to bring faster speed. The design process of the rising time and peak time neutrosophic membership functions should meet the following principles.

The parameters of the true, false, and uncertain membership functions should be selected in the range of short time. The smaller the response time requirement is, the larger the true value should be. The larger the response time requirement is, the larger the false value should be.

The system has relatively low requirements for the other four characteristics. So, the neutrosophic membership functions are designed as shown in Figure 14.

The desired speed is u_d = 5 rad/s. The simulation results are shown in Figure 15 and Table 3. It can be seen from Figure 15 that the speed can also converge to 5 rad/s. In Table 3, the rising time is 0.0006531 s and the peak time is 0.0013 s. The rising time and peak time are shorter than those in the above nonovershooting system. In other words, it has a faster response speed. But obviously, the overshoot ratio of the fast response system is increased to 16.1994%.

The iterative result of the population in the simulation is shown in Figure 16. It can be seen from Figure 16 that the convergence speed of this iteration population is faster. The average and optimal values of each generation are declining. The optimal value is also convergent and finally stabilizes at 0.1961.

4.2.3. Comprehensive Response System. The comprehensive response system expects to achieve a balance between response speed and overshoot indexes. The parameters of the overshoot ratio neutrosophic membership function in Figure 14 will be further reduced, thus increasing the limit of overshoot. The other five indexes' neutrosophic membership functions in Figure 14 are basically unchanged. So, the neutrosophic membership functions are designed as shown in Figure 17.

The desired speed is also u_d = 5 rad/s. The simulation results are shown in Figure 18 and Table 4. It can be seen from Figure 18 that the speed can converge to 5 rad/s. The overshoot index is obviously reduced than the fast response system and the response speed is also fast. In Table 4, the

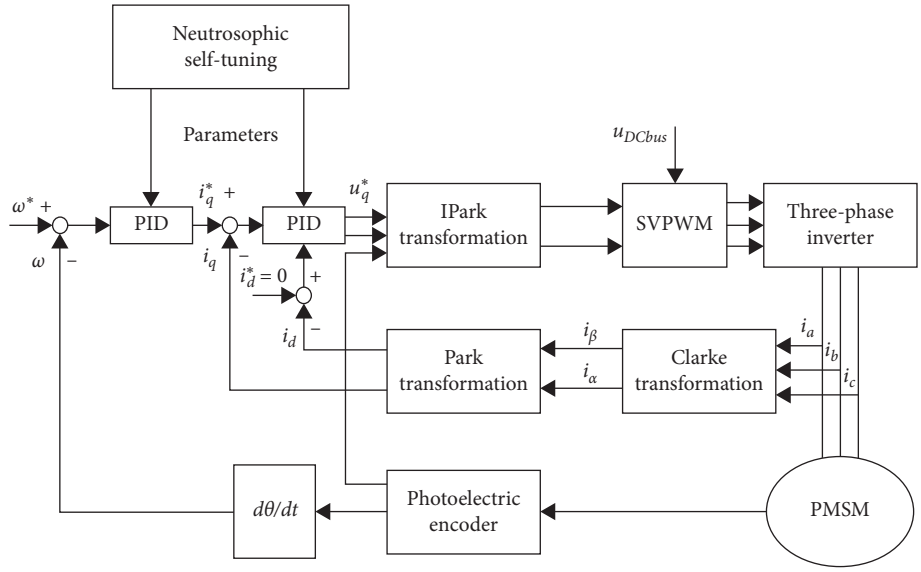

Figure 3: Structure diagram of the control system.

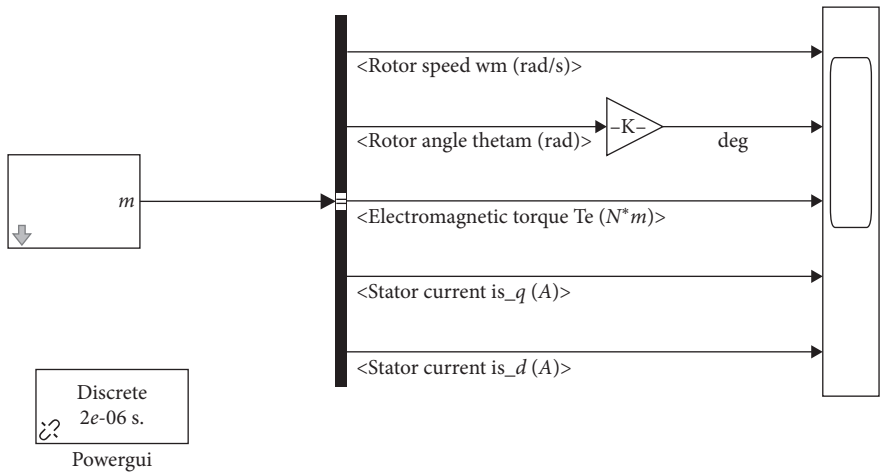

Figure 4: The diagram of the main control system.

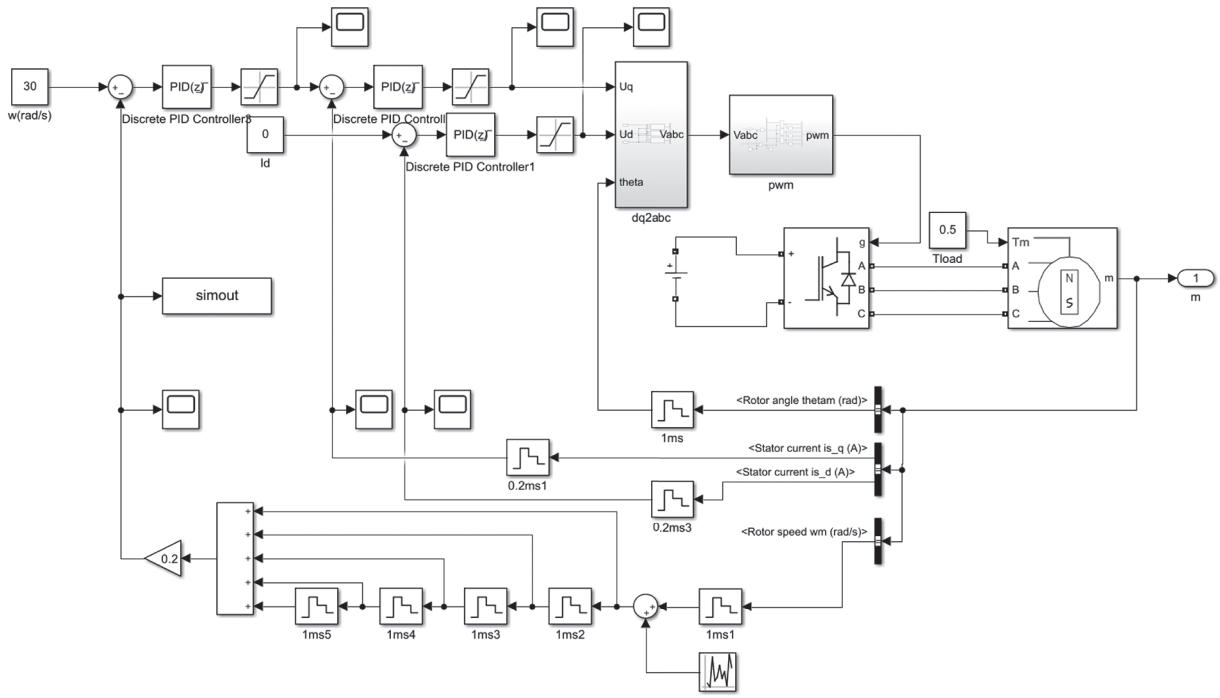

Figure 5: The diagram of the control subsystem.

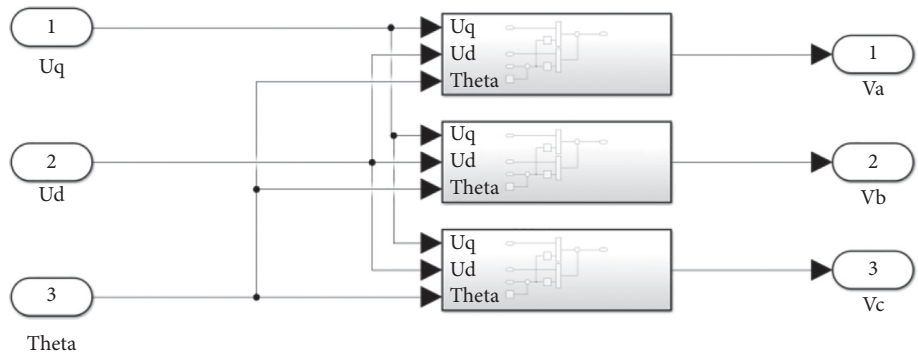

Figure 6: The diagram of two-phase DC to three-phase AC module.

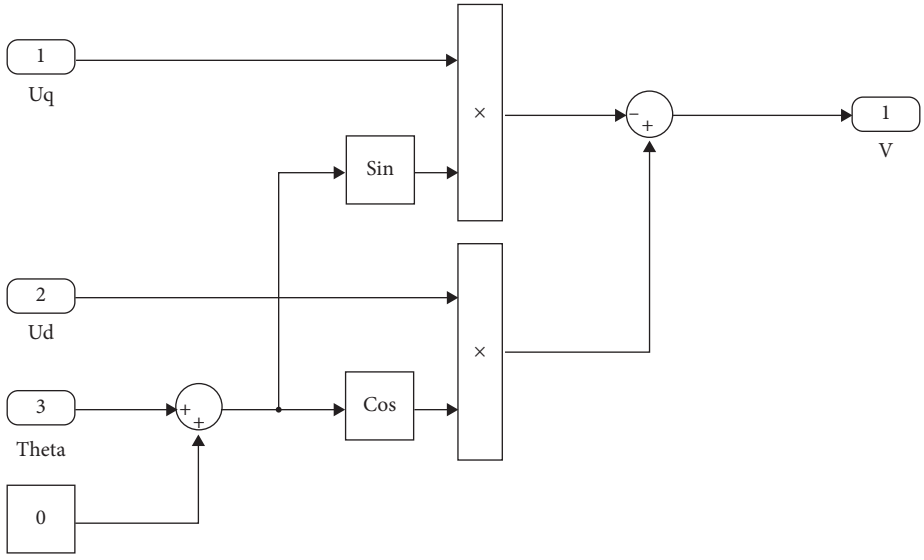

Figure 7: The first module in the two-phase DC to three-phase AC module.

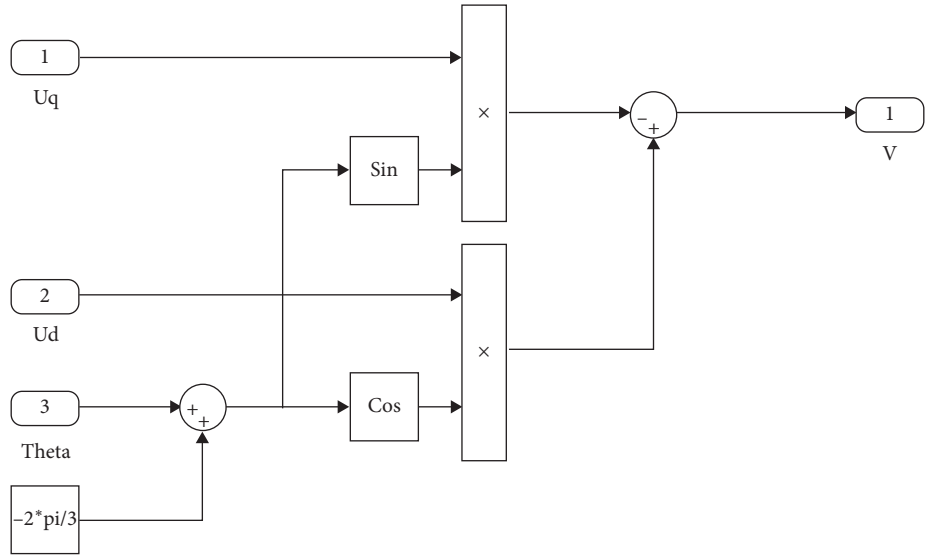

Figure 8: The second module in the two-phase DC to three-phase AC module.

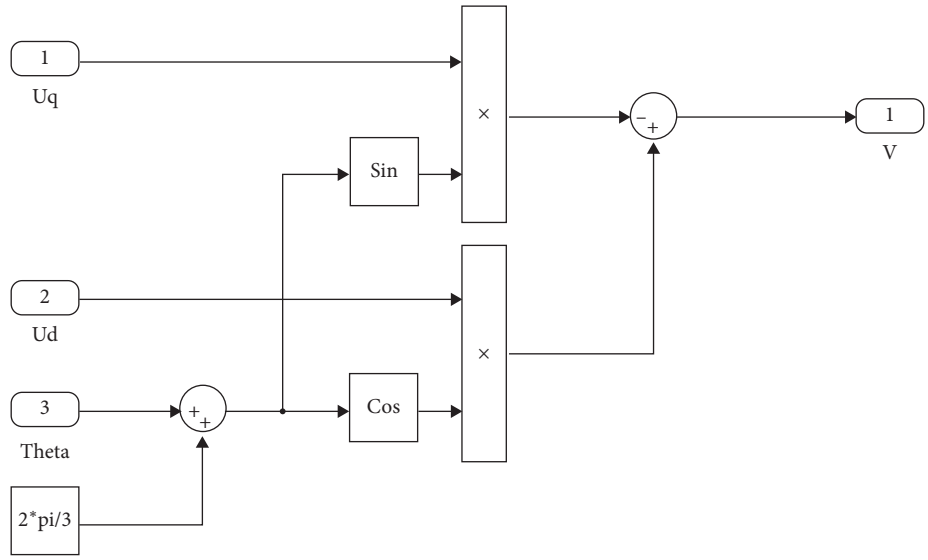

Figure 9: The third module in the two-phase DC to three-phase AC module.

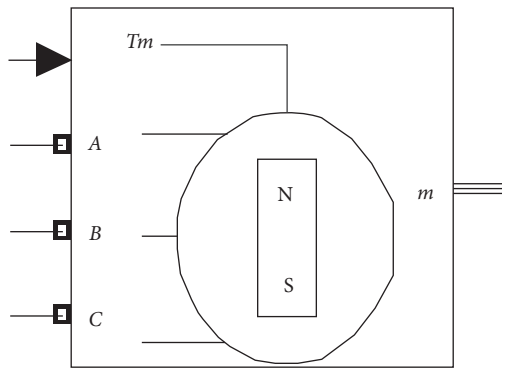

Figure 10: The PMSM used in simulations.

Table 1: Simulation parameters of PMSM.

Name	Value
Stator phase resistance	0.0485 Ω
Flux linkage	0.1194 Wb
d-axis inductance	0.1 mH
q-axis inductance	0.1 mH
Rated speed	1000 rpm
Rated power	100 W
Moment of inertia	0.0027 kgm^2
Viscous damping	0.0624924 F
Polar logarithm	1
Static friction	0

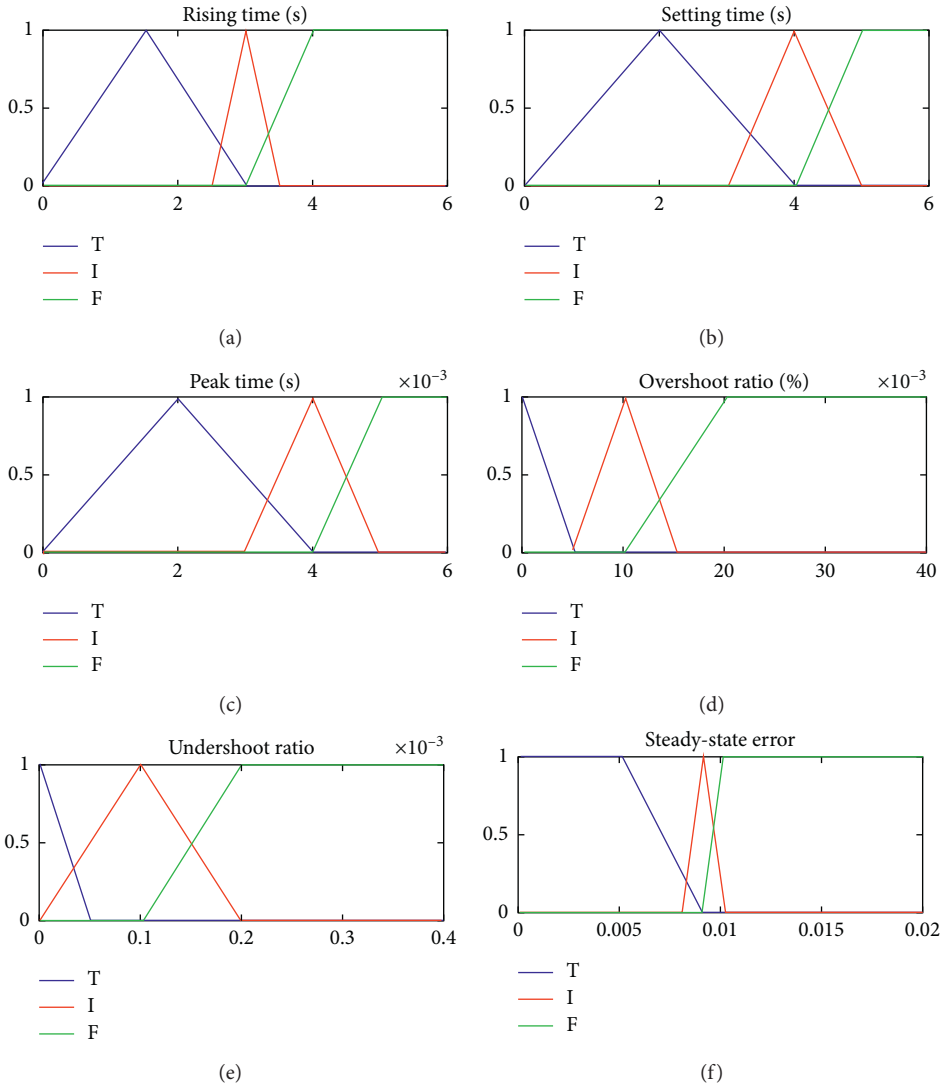

Figure 11: Neutrosophic membership function of nonovershooting system.

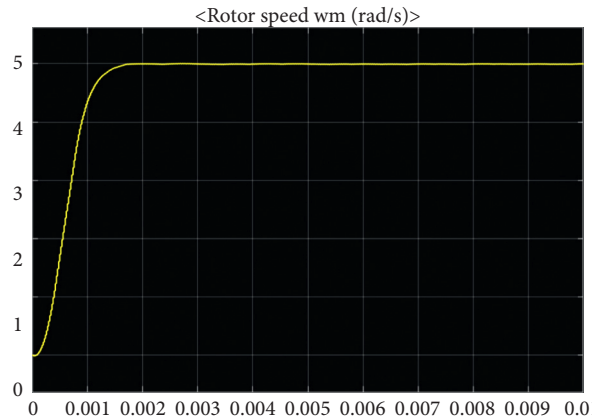

Figure 12: Simulation result of the nonovershooting system.

Table 2: Simulation results of the nonovershooting system.

Name	Value	Name	Value
Rising time	0.0007786s	p_1	53.9968
Settling time	0.0016s	i_1	2402.3231
Overshoot ratio	0%	p_2	194.1634
Undershoot ratio	0%	i_2	4275.5304
Peak time	0.0027s	Optimal value	0.0951
Stead-state error	0.0010	Running time	509.0194s

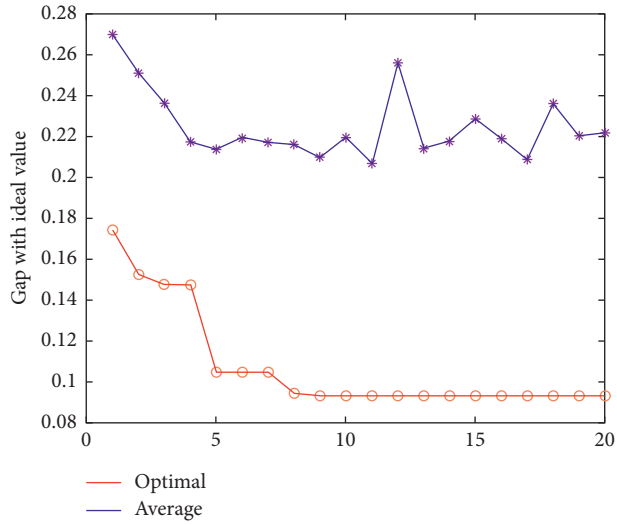

Figure 13: Population iterative of the nonovershooting system.

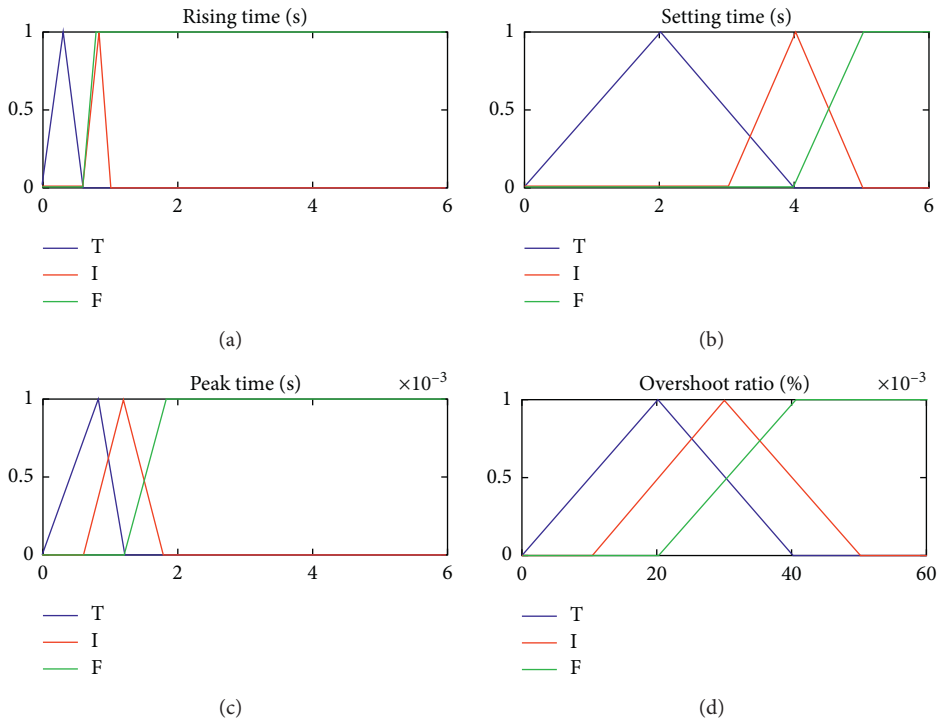

Figure 14: Continued.

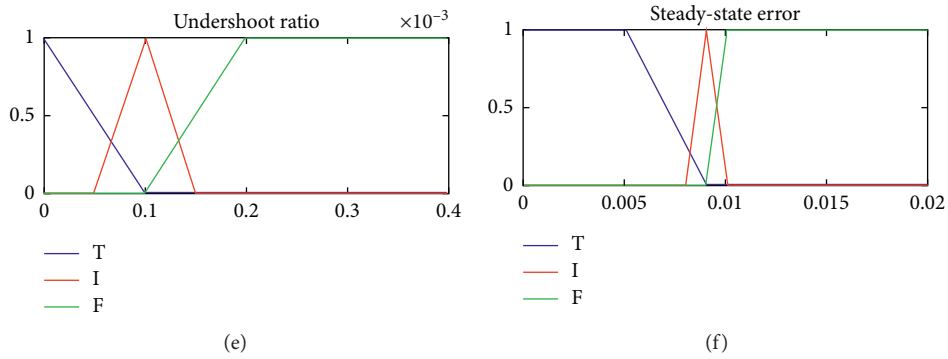

Figure 14: Neutrosophic membership function of the fast response system.

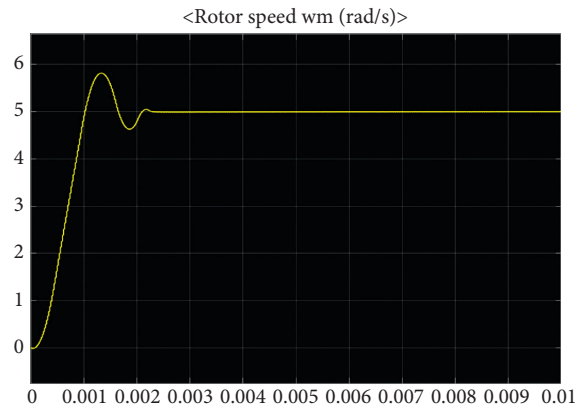

Figure 15: Simulation result of the fast response system.

Table 3: Simulation results of the fast response system.

Name	Value	Name	Value
Rising time	0.0006531 s	p_1	205.5004
Settling time	0.0020 s	i_1	2584.7556
Overshoot ratio	16.1994%	p_2	51.5292
Undershoot ratio	8.19%	i_2	8059.1018
Peak time	0.0013s	Optimal value	0.1961
Stead-state error	0.0013	Running time	707.9218 s

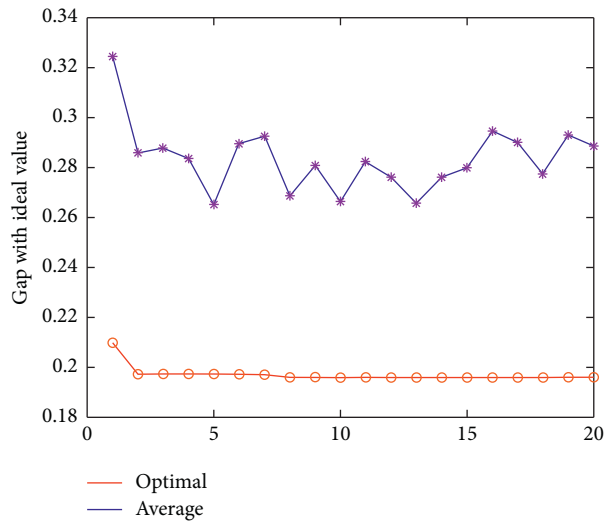

Figure 16: Population iterative of the fast response system.

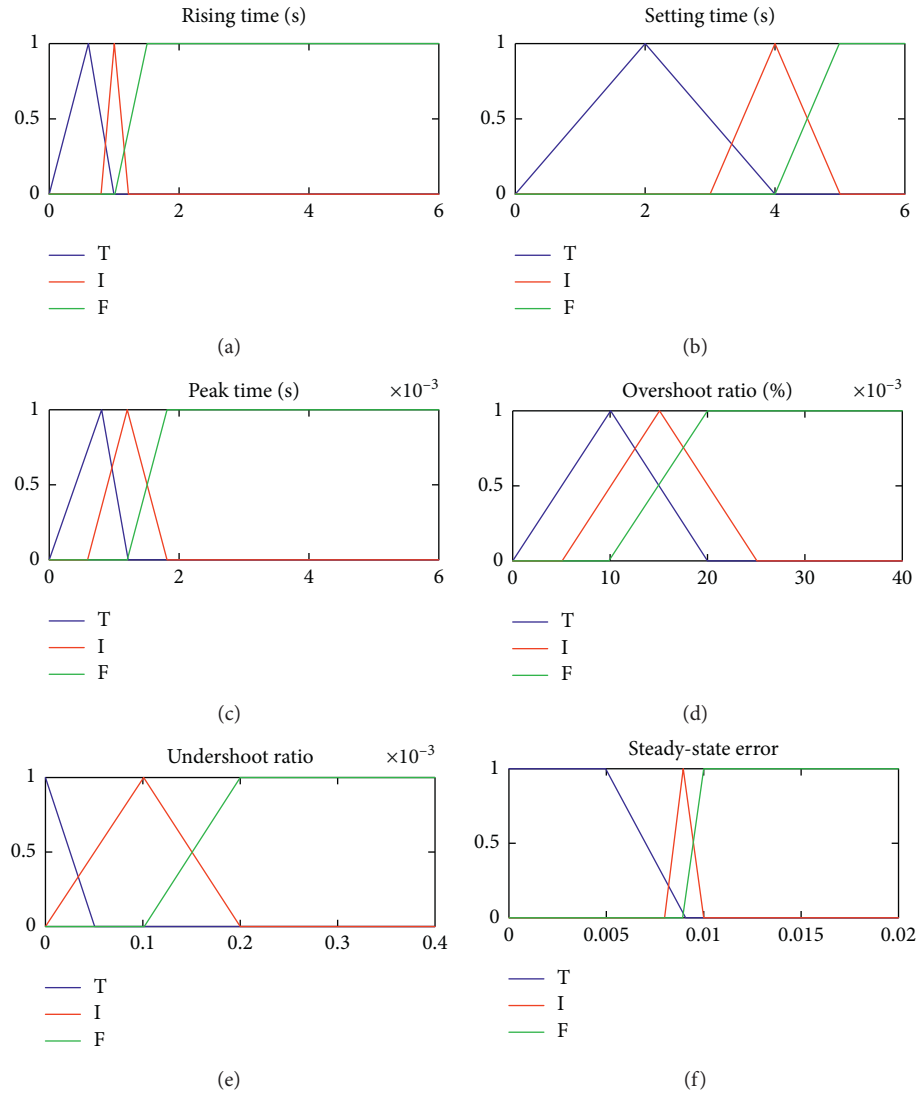

Figure 17: Neutrosophic membership function of comprehensive response system.

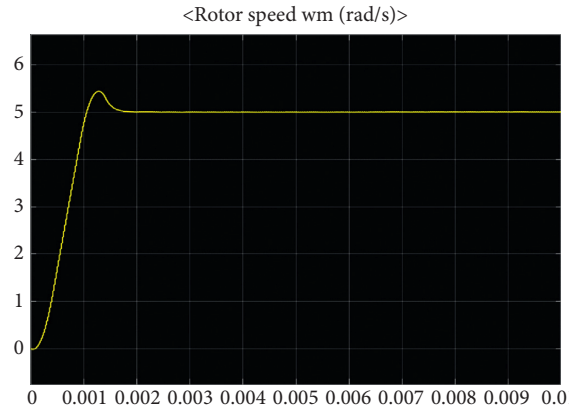

Figure 18: Simulation result of the comprehensive response system.

Table 4: Simulation results of the comprehensive response system.

Name	Value	Name	Value
Rising time	0.0006640 s	p_1	104.1265
Settling time	0.0015 s	i_1	2693.2360
Overshoot ratio	8.7895%	p_2	102.5041
Undershoot ratio	0%	i_2	8310.7028
Peak time	0.0013s	Optimal value	0.1741
Stead-state error	0.0017	Running time	690.9025 s

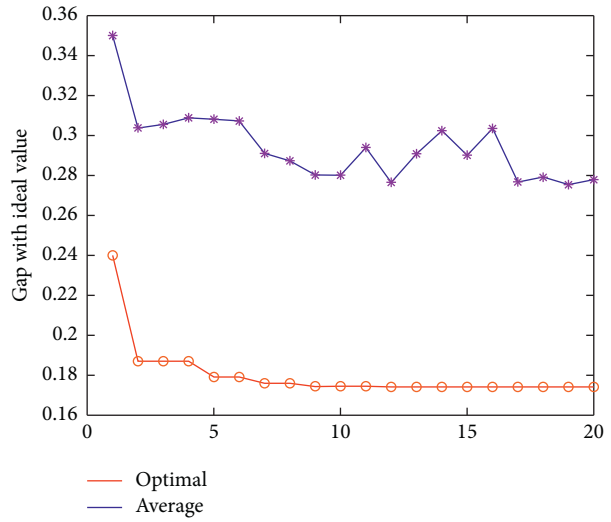

Figure 19: Population iterative of the comprehensive response system.

rising time is 0.000664 s and the peak time is 0.0013 s. The two time indexes are basically unchanged than the above fast response system. At the same time, the overshoot index is reduced from 16.1994% to 8.7895%.

The population iteration diagram is shown in Figure 19. The optimal value is also convergent and finally stabilizes at 0.1741.

5. Conclusion

In this paper, a neutrosophic self-tuning PID controller is designed for PMSM to match different characteristics. The neutrosophic membership functions of the designed controller can be adjusted according to different response requirements. Then the optimal parameters of the PID controller can be found based on the cosine similarity measure and genetic algorithm. Three kinds of AC permanent magnet motor control systems with different characteristics are designed in simulations. The results show that the designed controller can meet the requirements of different characteristics and has good control accuracy.

It is noted that the determination of the parameters of the six membership functions depends on certain expert experience. The different choices will directly affect the final PMSM control performance. In practice, it is difficult to choose the optimal membership parameters. In future research, the adaptive adjustment method of membership function parameters will be studied.

Data Availability

The data used to support the findings of this study are available from the corresponding author upon request.

Conflicts of Interest

The authors declare that there are no conflicts of interest regarding the publication of this paper.

References

[1] C. Jin and C. Zhou, "Application of permanent magnet variable frequency motor direct drive belt conveyor in coal mine," *Value Engineering*, vol. 37, no. 31, pp. 178-179, 2018.

[2] X. Sun, M. Wu, G. Lei, Y. Guo, and J. Zhu, "An improved model predictive current control for PMSM drives based on current track circle," *IEEE Transactions on Industrial Electronics*, vol. 68, no. 5, pp. 3782–3793, 2021.

[3] X. Sun, C. Hu, G. Lei, Z. Yang, Y. Guo, and J. Zhu, "Speed sensorless control of SPMSM drives for EVs with a binary search algorithm-based phase-locked loop," *IEEE Transactions on Vehicular Technology*, vol. 69, no. 5, pp. 4968–4978, 2020.

[4] X. Sun, J. Cao, G. Lei, Y. Guo, and J. Zhu, "Speed sensorless control for permanent magnet synchronous motors based on finite position set," *IEEE Transactions on Industrial Electronics*, vol. 67, no. 7, pp. 6089–6100, 2020.

[5] M. Hussein, "Modeling mechanical and electrical uncertain systems using functions of robust control MATLAB

Toolbox3," *International Journal of Advanced Computer Science and Applications*, vol. 6, no. 4, pp. 79–84, 2015.

[6] Y. V. Hote, D. R. Choudhury, and J. Gupta, "Robust stability analysis of the PWM push-pull DC-DC converter," *IEEE Transactions on Power Electronics*, vol. 24, no. 10, pp. 2353–2356, 2009.

[7] R. Precup and S. Preitl, "PI and PID controllers tuning for integral-type servo systems to ensure robust stability and controller robustness," *Springer Journal on Electrical Engineering*, vol. 88, pp. 149–156, 2006.

[8] H. Elkaranshawy, E. Bayoumi, and H. Soliman, "Robust control of a flexible-arm robot using Kharitonov theorem," *Electromotion*, vol. 16, pp. 98–108, 2009.

[9] F. Smarandache, *Neutrosophic Probability, Set, and Logic*, AMER Press, Rehoboth, DE, USA, 1998.

[10] H. Wang, F. Smarandache, Y. Zhang, and R. Sunderraman, "Single valued neutrosophic sets," *Multispace and Multistructure*, vol. 4, pp. 410–413, 2010.

[11] J. Ye, "A multicriteria decision-making method using aggregation operators for simplified neutrosophic sets," *Journal of Intelligent & Fuzzy Systems*, vol. 26, no. 5, pp. 2459–2466, 2014.

[12] L. Kong, Y. Wu, and J. Ye, "Misfire fault diagnosis method of gasoline engines using the cosine similarity measure of neutrosophic numbers," *Neutrosophic Sets and Systems*, vol. 8, pp. 43–46, 2015.

[13] J. Ye, "Fault diagnoses of steam turbine using the exponential similarity measure of neutrosophic numbers," *Journal of Intelligent & Fuzzy Systems*, vol. 30, no. 4, pp. 1927–1934, 2016.

[14] J. Ye, "Bidirectional projection method for multiple attribute group decision making with neutrosophic numbers," *Neural Computing and Applications*, vol. 28, no. 5, pp. 1021–1029, 2015.

[15] J. Ye, "Multiple-attribute group decision-making method under a neutrosophic number environment," *Journal of Intelligent Systems*, vol. 25, no. 3, pp. 377–386, 2016.

[16] W. Jiang and J. Ye, "Optimal design of truss structures using a neutrosophic number optimization model under an indeterminate environment," *Neutrosophic Sets and Systems*, vol. 14, pp. 93–97, 2016.

[17] J. Ye, "Neutrosophic linear equations and application in traffic flow problems," *Algorithms*, vol. 10133 pages, 2017.

[18] J. Chen, J. Ye, and S. Du, "Scale Effect and Anisotropy Analyzed for Neutrosophic Numbers of Rock Joint Roughness Coefficient Based on Neutrosophic Statisticsffect and anisotropy analyzed for neutrosophic numbers of rock joint roughness coefficient based on neutrosophic statistics," *Symmetry*, vol. 9, no. 10, p. 208, 2017.

[19] A. Bagis, "Determination of the PID controller parameters by modified genetic algorithm for improved performance," *Journal of Information Science and Engineering*, vol. 23, pp. 1469–1480, 2017.

[20] M. Olihin, L. Tack, and M. Kean, "Tuning of PID controller using particle swarm optimization (PSO)," in *Proceeding of the International Conference on Advanced Science, Engineering and Information Technology*, pp. 458–461, Bangi, Malaysia, January 2017.

[21] G. Malleham and A. Rajani, "Automatic tuning of PID controller using fuzy logic," in *Proceeding of the 8th International Conference on Development and Application Systems*, pp. 25–27, Jhongli, Taiwan, June 2006.

[22] M. Can and O. Ozguven, "PID tuning with neutrosophic similarity measure," *International Journal of Fuzzy Systems*, vol. 19, no. 2, pp. 489–503, 2017.

[23] J. Ye, "PID tuning method using single-valued neutrosophic cosine measure and genetic algorithm," *Intelligent Automation and Soft Computing*, vol. 25, no. 1, pp. 15–23, 2019.

[24] J. Ye and W. Cui, "Neutrosophic state feedback design method for SISO neutrosophic linear systems," *Cognitive Systems Research*, vol. 52, pp. 1056–1065, 2018.

[25] S.-Y. Ruan, J. Ye, and W.-H. Cui, "An improved PID tuning method by applying single-valued neutrosophic cosine, tangent, and exponential measures and a simulated annealing algorithm," *Neutrosophic Sets in Decision Analysis and Operations Research*, pp. 43–58, 2020.

[26] Y. Sun, Z. Wang, and F. Kong, *Design Guide of AC Servo System*, China Machine Press, Beijing, China, 2013.

[27] H. Mo, "Parameter analysis of permanent magnet AC servo motor," *Micromotor (Servo Technology)*, vol. 3, pp. 3–6, 2000.

[28] B. Xie and Y. Ren, *DSP Control Technology of Motor and its Application*, Beijing University of Aeronautics and Astronautics Press, Beijing, China, 2005.

[29] S. Lu, H. Wei, and K. Zhang, "Simulation analysis of PMSM vector control based on Matlab," *Industrial Control Computer*, vol. 24, no. 9, pp. 37–18, 2011.

[30] H. Mo, *Micro Motor*, China Electric Power Press, Beijing, China, 2015.

[31] F. Smarandache, "Neutrosophic probability, set, and logic," *Bulletin of the Transilvania University*, vol. 6, no. 41, pp. 41–48, 1999.

[32] J. Ye, "Improved cosine similarity measures of simplified neutrosophic sets for medical diagnoses," *Artificial Intelligence in Medicine*, vol. 63, no. 3, pp. 171–179, 2015.

[33] F. Huang, D. Liao, J. Li, H. Zhang, and Z. He, "PID complex parameter adjustment of UAV based on artificial intelligence," *Electromechanical Information*, vol. 24, pp. 85-86, 2018.